IMPACT RESISTANCE OF CARBON/EPOXY L-SECTIONS REINFORCED THROUGH-THE-THICKNESS BY TUFTING

Steve D. Green and Giuseppe Dell'Anno
The National Composites Centre, BS16 7FS Bristol, United Kingdom
steve.green@nccuk.com giuseppe.dellanno@nccuk.com
www.nccuk.com

Keywords: Textile Composite, Through-Thickness Reinforcement, Tufting, Stitching, Preforming

ABSTRACT

This paper provides an account of the experimental investigation into through-thickness reinforcement carried out at the National Composites Centre (NCC) (Bristol, UK). Single curvature preforms, reinforced through the-thickness with carbon fibre tufts, were impregnated via resin transfer moulding. Assessment of the quality of the manufactured parts via microscopy and CT scans showed excellent control over tuft location and alignment, as well as presence of cure-induced micro-cracks in the vicinity of the tufts. The mechanical response of tufted specimens under L-cantilever loading was compared to that of unreinforced controls, with the test set-up designed to introduce a combination of interlaminar tension and interlaminar shear stresses. While the control specimens failed in a brittle manner due to unstable delamination growth, the tufted specimens displayed a pseudo-plastic response, with gradual, progressive failure. Further mechanical testing of impacted specimens confirmed the remarkable capability of tufted composites to retain structural integrity following a 16 J impact.

1. INTRODUCTION

Three-dimensional fibre architectures offer the potential to address composites susceptibility to delamination, therefore providing components with increased damage tolerance and impact resistance compared to the two-dimensional counterparts. Dry preforms with yarns arranged spatially in a 3D fashion rather than only across the main plane of the component can be manufactured either by three-dimensional weaving methods using specially designed looms [1], or by adding a given amount of discrete reinforcing elements to link physically adjoining fibrous layers to each other. The latter approach allows the reinforcement through-the-thickness of otherwise conventional 2D preforms, with the insertion of Z-pins [2], stitches [3] or tufts [4] (sometime referred to as *micro-fasteners*) only in those selected sections of the composite with high out-of-plane stress state. Once a three-dimensional fibre architecture is obtained, delamination or debonding in the Z-reinforced areas requires the pull-out or breakage of such micro-fasteners [5, 6, 7, 8, 9].

The 'local' approach to 3D reinforcement offers obvious advantages compared to the 'integral' approach in terms of flexibility and versatility of applications: most of the local 3D reinforcement technologies can be implemented into existing manufacturing processes with relatively small modifications or upgrades of the pre-existing tooling and setups. Also, experimental findings and model analysis often show that there is rarely the need for reinforcing the whole of a structure. An optimised design would locate reinforcement in the areas most susceptible to delamination or impact damage, minimising the cost and avoiding affecting the whole part with the drawbacks that any reinforcing technique necessarily implies.

Broadly speaking, most local 3D reinforcement methods fit one of two main categories, pinning or some form of stitching, depending on whether the preform to be reinforced is in the pre-impregnated or dry, respectively.

A modified form of stitching, tufting is one of the simplest methods of local TTR introduction, involving the insertion of a single thread through the full thickness of a preform via a needle, generating a loop on the rear surface of the preform. Access is required only to a single side of the preform, while this is supported on either specialised rigs or sacrificial substrates, as shown in Figure 1.

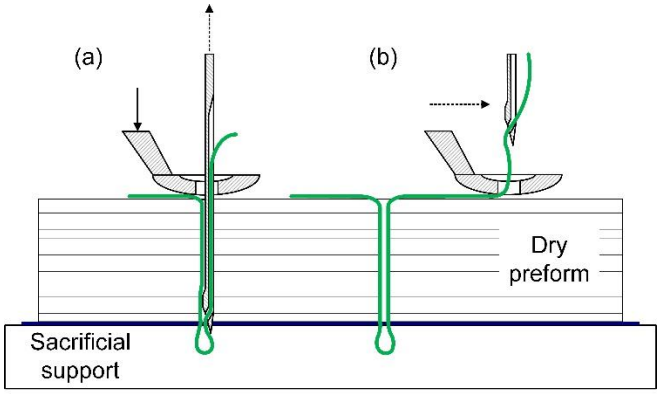

Figure 1: Schematic of tufting process: tuft (in green) being inserted (a) and fully inserted (b).

Although one of the earliest examples found in the literature of tufting technology applied to the composite field dates back to 1973 [10], it is only recently that tufting machines for composite applications have been made available on the market and the technology is slowly creeping in the production environment.

Some technical information on the tufting process itself is available in the published literature [11, 12] as well as some general comparisons of tufting against other forms of stitching [13] or other forms of Z-direction reinforcement [14, 15]. The earliest systematic work aiming at quantifying the mechanical performance of tufted composites was completed in Cranfield University in 2007 [16]. Assessment of the mechanical properties of tufted composites confirmed that the effects of tufting on the performance of the cured composite were similar to those of stitching. In particular, a significant increase in G_{Ic}, a lesser but still significant increase in G_{IIc} [17, 18] were noted, as well as improvements in the compression-after-impact behaviour [19]. Such results were confirmed both in quasi-static configurations and at higher delamination rates [20, 21].

More attention has been devoted recently to the industrial manufacturing aspects related to the production of tufted components, with emphasis on the clear definition of the technology envelope, the design of the required supporting rigs and tools, and the identification of a suitable impregnation strategy [4]. The research work to date has identified some challenges in the processing of complex geometry components, the work reported here highlights some initial findings on the manufacturing and assessment of single-curvature, relatively thick elements.

2. MANUFACTURE

Two sets of specimens were manufactured from dry preforms via resin transfer moulding (RTM), using custom tooling. A back pressure of 4 bar absolute was used during this process. The specimens featured 85 mm long arms and an internal radius of 13 mm, while the laminate thickness was 10 mm with a specimen width of 10 mm. Both sets of specimens were made out of commercially available carbon fibre fabric, woven in a 2x2 twill pattern, based on 12k T700SC filament yarns. The plies were laid-up as $[0°]_{16}$ laminate, with the balanced woven fabric producing a biaxial laminate with an equal distribution of 0° and 90° fibres. All preforms were injected with Cytec CYCOM 890 RTM epoxy resin and cured at 180 °C. While the first set of specimens was impregnated to produce a baseline 2D control, the second featured through-the-thickness reinforcement (TTR) in the form of carbon fibre tufts, which generated a local 3D fibre architecture.

The preforms were tufted at the NCC using a KSL RS522 tufting tool interfaced to a KUKA KR240-180L robot. The robot was programmed to insert the highly twisted, double yarn thread supplied by Schappe, perpendicular to the mean plane of the L-sections (see Figure 2). The 4k carbon fibre tufts were arranged in a square array with 4mm spacing, resulting in a tuft areal density of 0.96%. The preform was supported on a tufting tool featuring sacrificial foam inserts covered in layer of release film to allow insertion of needle and thread through the full preform thickness.

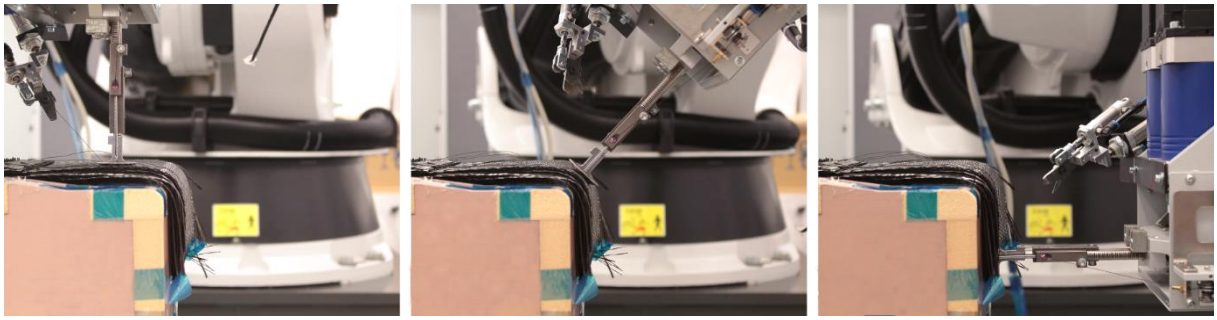

Figure 2: Control of tufting head around L-section radius, with needle penetrating the top flat section of the L profile (left), the corner apex (centre), and the bottom flat section (right). The base of the articulated KUKA robot is visible in the background.

3. SPECIMEN CHARACTERISATION

Optical microscopy was used for the characterisation of the internal reinforcement architecture, with representative polished cross sections shown in Figure 3. No visible voids or cracks were detected in the control specimen. The layers show some evident out-of-plane waviness which is due to the inherent crimp of the woven fabric. The section of the tufted specimen shows accurate and repeatable tuft insertions over the curved geometry. Each individual tuft is aligned to the orthogonal out-of-plane direction with equal spacing between the adjacent TTR elements. This is in direct contrast to experimental observation on Z-pinned components, which, even on flat laminates, demonstrate stochastic variation in alignment with typical misalignment angles of 10-25° [22] [23].

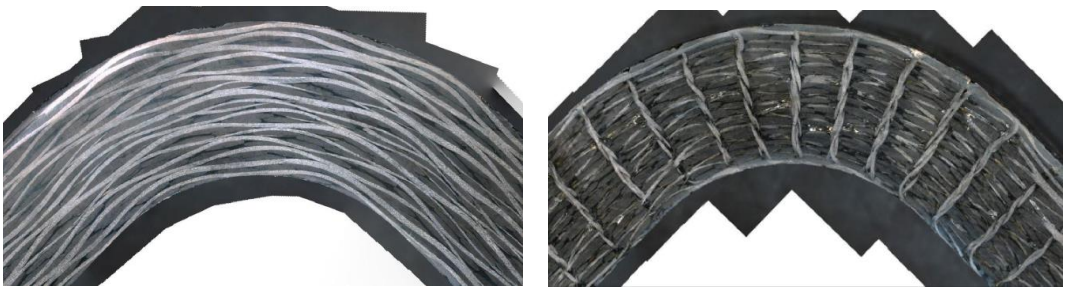

Figure 3: Polished cross-section microscopy images of as-manufactured L-section specimens. Control on the left and tufted on the right.

Micro computed tomography (CT) scanning was used to characterise internal defects in the as-manufactured specimens. Prior to CT scanning, samples were soaked in a zinc iodide dye penetrant to highlight any cracks or voids connected to the surface. Representative images of the control and tufted sections, including the full width of the specimens, are shown in Figure 4.

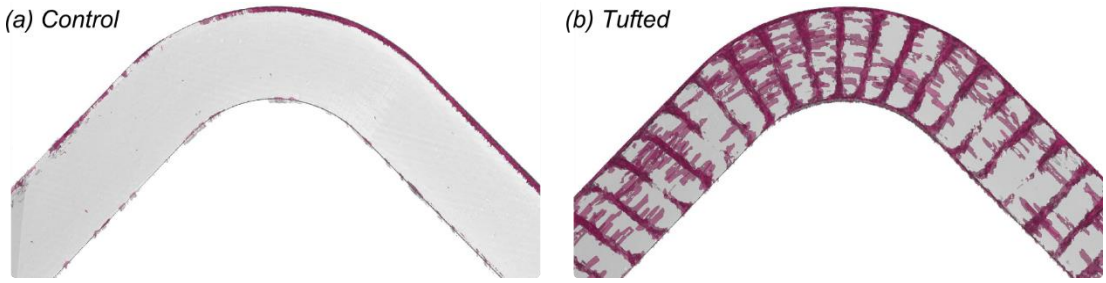

Figure 4: Images from CT scans of as-manufactured control (a) and tufted (b) L-section specimens through full specimen width, showing defects highlighted by dye penetrant in pink.

Consistent with the findings of the microscopy, no detectable defects were reported in the control specimen. The dyed layer on the surface is due to residual dye penetrant which could not be removed completely from the specimen after soaking. However, the tufted specimens appeared affected by a noticeable amount of defects along the tufts length, occasionally extending into the base laminate. A more detailed view of these defects was obtained from further CT scanning and optical microscopy, shown in Figure 5.

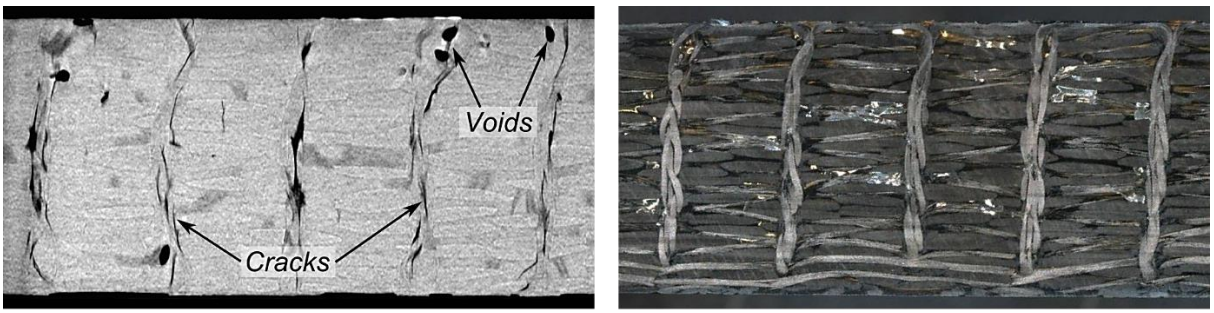

(a) CT scan (no dye penetrant) (b) Microscopy

Figure 5: Details of defects seen in tufted specimens through CT scanning (a) and optical microscopy (b).

Some voids were observed in and around the tufts, particularly close to the surfaces of the laminate, however, most of the indicated defects were cure-induced micro-cracks.

The lighter regions in the microscopy image in Figure 5(b) are reflections from resin cracks behind the plane of the cut. These cure-induced micro-cracks occur since the tufts constrain the through-thickness contraction of the laminate occurring due to resin shrinkage and thermo-elastic cooldown effects. The resulting residual stresses can lead to crack formation in the material. Similar defects have been observed experimentally and predicted with finite element simulations in orthogonal 3D woven composites [24]. These materials have a nominally similar reinforcement architecture to the tufted specimens considered here, with binder yarns orientated directly in the through-thickness direction. Similarly, nominally orthogonally orientated Z-pins have been observed to become partially of fully debonded from the base laminate. Finite element simulations confirm that this is due to residual stresses formed during manufacture [25] [26] with a numerical parametric study suggesting that some debonding of the TTR element must be expected when manufacturing high temperature curing laminates reinforced with carbon fibre Z-pins [25].

4. MECHANICAL TESTING

4.1. Procedure

4.1.1. Impact test

For each reinforcement type, a set of four specimens were tested in their as-manufactured state, with three remaining specimens tested for residual strength after impact to determine the effect of TTR on the damage tolerance of the structure.

Impact tests were conducted in an Instron Dynatup 9250 HV instrumented impact tower, with specimens secured in a bespoke fixture supporting both of their ends, as shown in Figure 6. A 10 mm radius steel hemispherical impactor impacted the apex of the external radius with an energy of 16J. Each impact event was monitored to verify consistency. The load measured by the load-cell at the back of the impactor was recorded; some representative load traces are shown in the plots of Figure 7. Post-processing of the load data allowed estimation of the total impact energy absorbed by the specimen; a scatter among specimens of less than 1.5% was observed.

Figure 6: Specimen loaded in impacting rig.

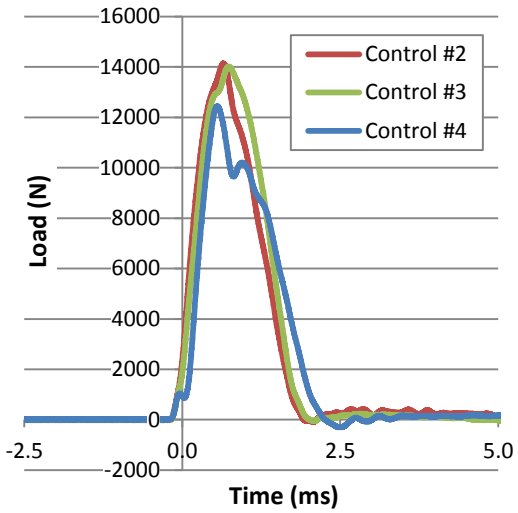

Figure 7: Load vs time plots for impacting of control specimens.

4.1.2. L-cantilever test

The L-cantilever rig geometry is shown in Figure 8. The L-section specimens were prepared after machining by coarse polishing on one side and fine polishing on the other for characterisation by optical microscopy. The specimen geometry is broadly similar to that used in curved beam strength testing (ASTM 6415), where the load introduction via four point bending generates a state of pure bending in curved region, producing out-of-plane tensile stresses. The L-cantilever rig differed by fixturing the specimen via a clamp at one end, and load introduction via a cylindrical ended shaft of 12.5 mm radius. The more complex stress state this produces is a better representation of a practical engineering application. Mechanical testing was conducted in a Roell Amsler HCT 25 kN load cell at a loading rate of 2 mm/min.

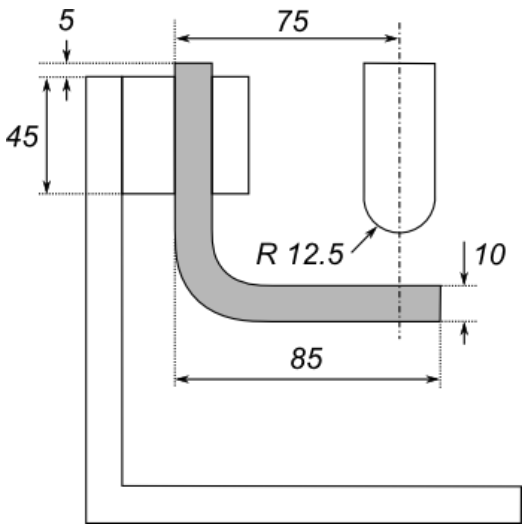

Figure 8: Schematic of the L-cantilever test setup.

4.2. Results

4.2.1. Impact test

The specimens previously CT scanned to visualise as-manufactured defects were re-infiltrated with dye penetrant and CT scanned after impacting. The reconstructed 3D images of the impacted specimens

in Figure 9 can be compared with those in Figure 4, whereby any additional damage can be directly attributed to the impact event.

The control specimen showed a significant number of delaminations after impact throughout the whole thickness of the laminate, with a few cracks running far from the radius region down a side arm. Although a significant number of defects from manufacture were present in the tufted specimen, the tufts were effective in the reducing the number impact-induced delaminations and arrested their progression away from the site of the impact.

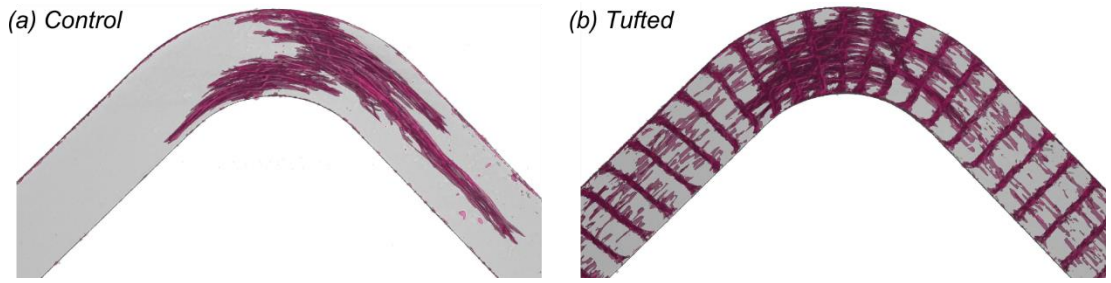

Figure 9: Images from CT scans of impacted control (a) and tufted (b) L-section specimens through full specimen width, showing defects in pink.

4.2.2. L-cantilever test

Representative load curves from the L-cantilever testing are shown in Figure 10. Considering first the behaviour of the as-manufactured specimens, both the control and tufted specimens displayed an approximately linear load response up until the first point of failure. Slight non-linearity is to be expected due to geometric non-linearity of the structure as it opens up under loading and does not necessarily indicate non-linear material response. However, the stiffness of the tufted specimens was 5% lower than the control as the introduction of tufts reduces in-plane properties, mainly due to the development of in-plane waviness in the base laminate. This value should be considered indicative only since it is not significantly greater than the standard deviation of each sample set.

Damage initiation in the specimens was not modified by the addition of tufts, in fact, the control specimens sustained a higher initiation load. The onset of failure in the control specimens showed an immediate sharp load drop to a low level of base load (85% reduction in peak load) as a result of unstable propagation of the delamination cracks. However, while the initial peak was lower than the control, the tufted specimens showed continued load carrying capability approximating a plateau region followed by a gradual drop in load. This indicates stable delamination and crack growth in these specimens, absorbing a significant level of energy and producing a pseudo-plastic response.

These findings are consistent with previous experimental work [27] [15] and finite element analysis studies [28] [29] which show that TTR of various types do not improve the delamination initiation properties of reinforced composites. TTR elements are highly effective at delaying the propagation of delaminations via the development of a crack bridging zone, alleviating the stresses at the crack tip and absorbing energy through pull-out. However, a crack bridging zone only develops once a crack of several millimeters in length has formed in the vicinity of the TTR element.

The damage resulting from the impact to the control specimens translated into significantly reduced stiffness, and peak load reduction of 81%. The results for the impacted tufted specimens were strikingly different, with a small reduction in initial stiffness compared to the as-manufactured specimens, followed by a non-linear softening response in the initial region of the load curve. The peak load of the impacted tufted specimens were within just 6% of the as-manufactured specimens and again produced a graceful pseudo-plastic failure.

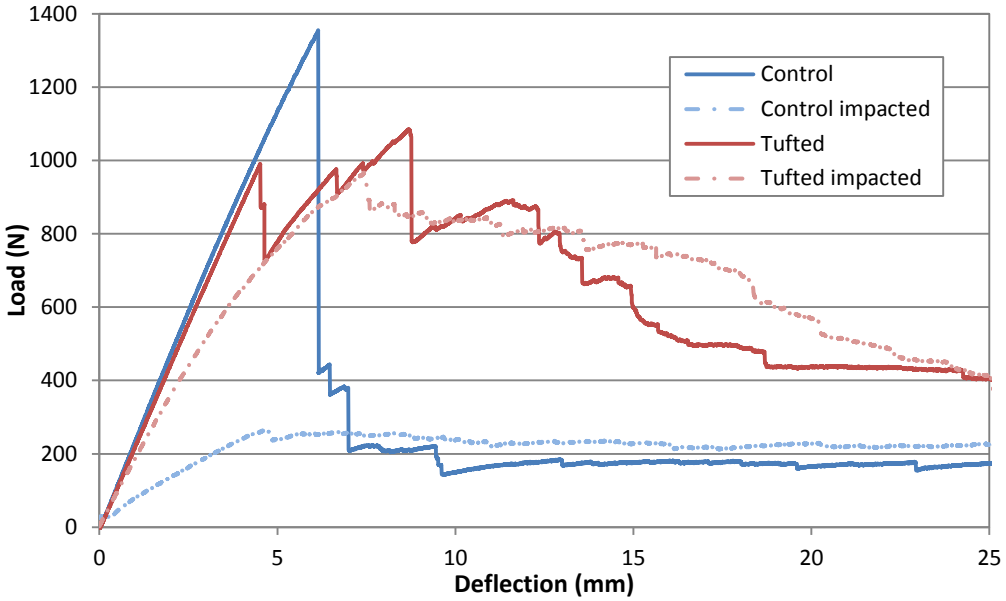

Figure 10: Representative load-deflection curves for as-manufactured and impacted specimens.

Load values from each dataset are summarised in Figure 11. Note that the initiation loads shown here do not account for the non-linearity shown in the impacted tufted specimens as no clearly identifiable load drop was apparent until close to the ultimate load. It is not completely clear whether this non-linearity is because the impact damaged structure exhibits geometrical non-linearity under loading as cracks open up (but do not propagate) or because further damage is progressively accumulating. Further analysis of partially loaded specimens would be necessary to clarify this.

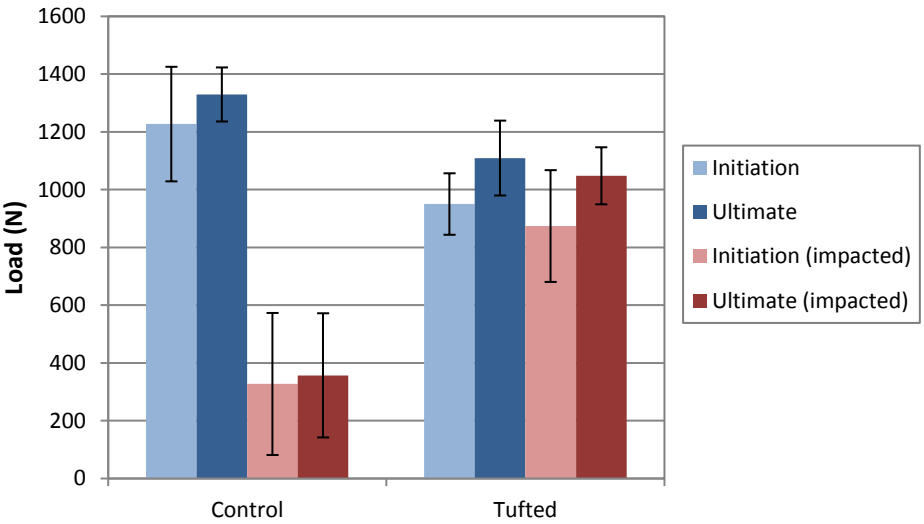

Figure 11: Chart summarising load values sustained for each reinforcement type (error bars represent one standard deviation).

5. FAILURE ANALYSIS

Microscopy images of the (non-impacted) L-section specimens after mechanical testing are shown in Figure 12. The 2D control specimen shows a high density of cracks and delaminations, some of which have spread far beyond the radius region. Conversely, the 2D tufted specimen showed delaminations which were much more localised to the radius region as well as a shift in the final failure mechanism to compressive fibre failure on the outer surface of the specimen close to the clamp. This 2D tufted specimen was subsequently CT scanned to provide a more detailed picture of the internal damage and failure mechanisms, with Figure 13 clearly illustrating the bridging action of the tufts. Many of the tufts

have fractured close to the concave surface of the section but continue to provide bridging forces and absorb energy upon further loading due to friction during pull-out. Some of the tufts have two points of fracture demonstrating that a significant tensile load can still be carried by the tuft after its initial fracture.

Tufts were inserted throughout the loaded region of the L-section; starting just inside the clamped region and continuing beyond the contact with the shaft in order to prevent failure occurring just outside the region of the tufting. However, tufts beyond the crack tip would have had no effect on the crack propagation. The effectiveness of tufts confining delaminations to a localised region suggests that the outer rows could be removed, reducing the time and cost of tuft insertion while providing the same mechanical benefits. While tufting may reduce in-plane stiffness and strength, strain to failure is unaffected [30] so targeted use of tufting in a structure only at critical locations could pose a minimal impact to in-plane properties.

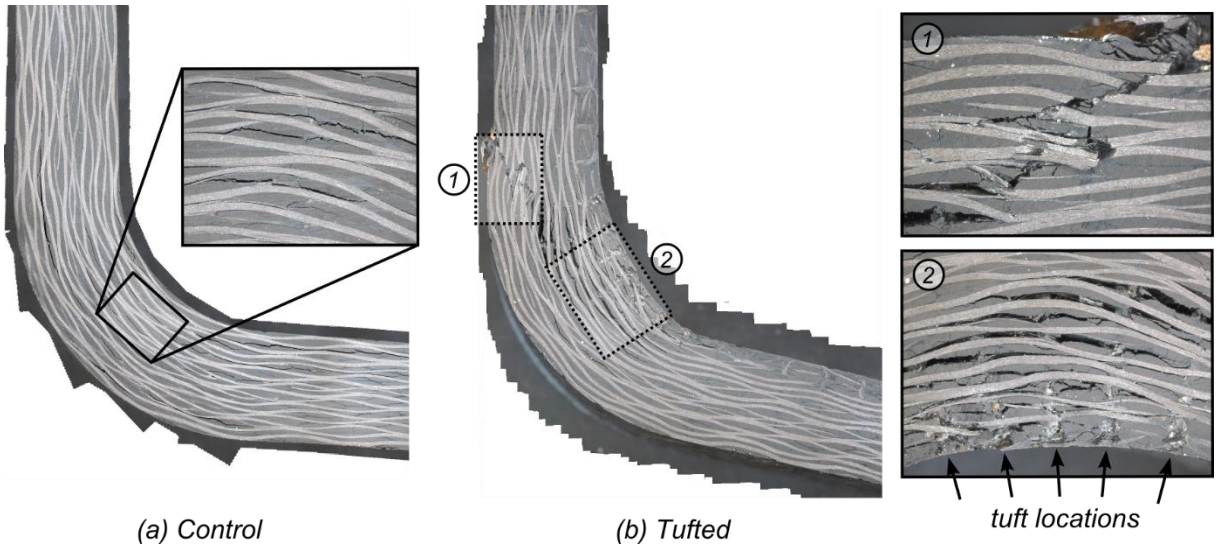

Figure 12: Microscopy images of failed L-section specimens (non-impacted), shown orientated as in loaded in L cantilever rig (see Figure 8).

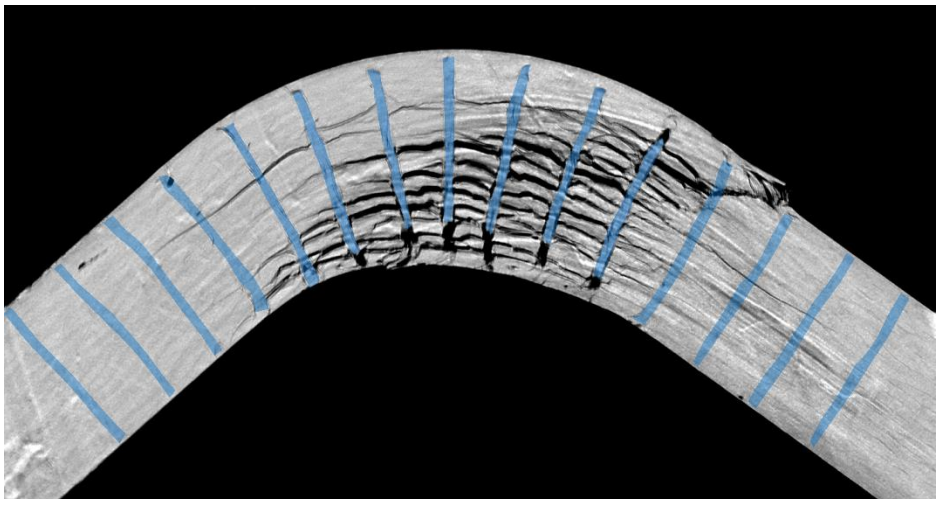

Figure 13: CT scan image of failed 2D tufted specimen (non-impacted), highlighting tufts in blue.

6. CONCLUSIONS

A set of specimens featuring through-thickness reinforcement via tufting were manufactured successfully via RTM. Good quality tuft insertion was achieved, with precise positioning around a radius and small loops on the back face. Detailed analysis of cured parts via optical microscopy and CT scans showed some defects in the form of cure-induced micro-cracks.

L-cantilever testing showed that tufting did not improve the failure initiation load of the specimens, in agreement with the existing literature. However, the tufted L-sections provided significantly improved energy absorption with progressive pseudo-plastic failure, compared to the brittle failure of the unreinforced control. The extent of impact-induced micro-cracks and delaminations was much reduced and localised in the tufted specimens. These also showed remarkable post-impact properties with only a minor knock down in strength after impact compared to a catastrophic loss of load carrying capability in the 2D control. The key mechanism for both limiting impact damage and the pseudo-plastic mechanical response was shown to be bridging of delamination cracks. Further improvements in the response of tufted composites can be expected since the TTR pattern cannot yet be considered optimised. This would include more efficient use of reinforcing elements only where required to minimise the manufacturing effort and reduce potential detrimental effects.

It is currently unclear how detrimental the micro-cracks in the tufted specimens are, since the tufts greatly increased the damage tolerance of the laminate, at least in terms of suppressing delaminations. However, these cracks could propagate as non-catastrophic intraply cracks. Certainly, as shown by the ingress of dye-penetrant, these cracks could facilitate absorption of moisture or other liquids into the laminate. Strategies for mitigating or altogether avoiding the formation of micro-cracks in the vicinity of the TTR elements are currently being investigated and are expected to facilitate further the transition of the tufting technology into industrial and production environments.

REFERENCES

[1] P. Potluri, P. Hogg, M. Arshad, D. Jetavat and P. Jamshidi, "Influence of fibre architecture on impact damage tolerance in 3D woven composites," *Applied Composite Materials,* vol. 19, pp. 799-812, 2012.

[2] I. K. Partridge, D. D. R. Cartié and T. Bonnington, "Manufacture and performance of z-pinned composites," in *Advanced Polymeric Materials*, Boca Raton, Florida: CRC Press, 2003, pp. 151-137.

[3] E. Greenhalgh and M. Hiley, "The assessment of novel materials and processes for the impact tolerant design of stiffened composite aerospace structures," *Composites Part A: Applied Science and Manufaturing,* vol. 34, pp. 151-61, 2003.

[4] G. Dell'Anno, J. W. G. Treiber and I. K. Partridge, "Manufacturing of composite parts reinforced through-thickness by tufting (Article in press)," *Robotics and computer-integrated manufacturing,* vol. 37, pp. 262-272, 2016.

[5] A. P. Mouritz, M. K. Bannister, P. J. Falzon and K. H. Leong, "Review of applications for advanced three-dimensional fibre textile composites," *Composites Part A: Applied Science and Manufacturing,* vol. 30, no. 12, pp. 1445-1461, 1999.

[6] L. C. Dickinson, G. L. Farley and M. K. Hinders, "Translaminar reinforced composites: A review," *Journal of Composites Technology and Research,* vol. 21, no. 1, pp. 3-15, 1999.

[7] I. K. Partridge and D. D. R. Cartié, "Delamination resistant laminates by Z-fiber(R) pinning: Part I manufacture and fracture performance," *Composites Part A: Applied Science and Manufacturing,* vol. 36, no. 1, pp. 55-64, 2005.

[8] K. A. Dransfield, C. Baillie and Y. W. May, "Improving the delamination resistance of CFRP by stitching: A review," *Composites Science and Technology,* vol. 50, no. 3, pp. 305-17, 1994.

[9] A. P. Mouritz, "Review of Z-pinned composite laminates," *Composites Part A: Applied Science and Manufacturing,* vol. 38, no. 12, pp. 2383-2397, 2007.

[10] D. W. Bauer and W. V. Kotlensky, "Relationship between structure and strength for CVD carbon infiltrated substrates. Part 2: Three dimensional woven, tufted and needled substrates," *SAMPE Quarterly,* vol. 4, no. 2, pp. 10-20, 1973.

[11] R. Keilmann, "Innovative processing techniques for carbon fibre materials," *JEC Composites,* vol. 5, pp. 81-82, 2003.

[12] G. F. Turner, "New flexible robotic composite stitching," *Advanced Materials & Composite News,* vol. 23, no. 516, p. 6, 2001.

[13] J. Wittig and F. Rattay, "Robotic three-dimensional stitching technology," in *46th International SAMPE Symposium*, Long Beach, California, 6-10 May 2001.

[14] J. Brandt, A. Geßler and J. Filsinger, "New approaches in tectile and impregnation technologies for the cost effective manufacturing of CFRP aerospace components," in *23rd International Congress of Aeronautical Sciences*, Toronto, Canada, 2002.

[15] D. D. R. Cartié, G. Dell'Anno, E. Poulin and I. K. Partridge, "3D reinforcement of stiffener-to-skin T-joints by Z-pinning and tufting," *Engineering Fracture Mechanics,* vol. 73, pp. 2532-2540, 2006.

[16] G. Dell'Anno, "Effect of tufting on the mechanical behaviour of carbon fabric/epoxy composites [PhD dissertation]," Cranfield University, Cranfield, UK, 2007.

[17] J. W. G. Treiber, "Performance of tufted carbon fibre/epoxy composites [PhD dissertation]," Cranfield University, Cranfield, UK, 2011.

[18] M. Colin de Verdiere, A. K. Pickett, A. A. Skordos and V. Witzel, "Evaluation of the mechanical and damage behaviour of tufted non crimped fabric composites using full field measurements," *Composites Science and Technology,* vol. 69, pp. 131-138, 2009.

[19] G. Dell'Anno, D. D. R. Cartié , I. K. Partridge and A. Rezai, "Exploring mechanical property balance in tufted carbon fabric/epoxy composites," *Composites Part A: Applied Science and Manufacturing,* vol. 38, no. 11, pp. 2366-2373, 2007.

[20] M. Colin de Verdiere, A. A. Skordos, M. May and A. C. Walton, "Influence of loading rate on the delamination response of untufted and tufted carbon epoxy non crimp fabric composites: Mode I," *Engineering Fracture Mechanics,* vol. 96, pp. 11-25, 2012.

[21] M. Colin de Verdiere, A. A. Skordos, A. C. Walton and M. May, "Influence of loading rate on the delamination response of untufted and tufted carbon epoxy non crimp fabric composites/More II," *Engineering Fracture Mechanics,* vol. 96, pp. 1-10, 2012.

[22] M. Yasaee, J. K. Lander, G. Allegri and S. R. Hallett, "Experimental characterisation of mixed mode traction–displacement relationships for a single carbon composite Z-pin," *Composites Science and Technology,* vol. 94, no. 9, pp. 123-131, 2014.

[23] P. Chang, A. P. Mouritz and B. N. Cox, "Properties and failure mechanisms of z-pinned laminates in monotonic and cyclic tension," *Composites Part A: Applied Science and Manufacturing,* vol. 37, no. 10, pp. 1501-1513, 2006.

[24] I. Tsukrov, H. Bayraktar, M. Giovinazzo, J. Goering, T. Gross and M. Fruscello, "Finite Element Modeling to Predict Cure-Induced Microcracking in Three-Dimensional Woven Composites," *International Journal of Fracture,* pp. 1-8, 2012.

[25] R. D. Sweeting and R. S. Thomson, "The effect of thermal mismatch on Z-pinned laminated composite structures," *Composite Structures,* vol. 66, pp. 189-195, 2004.

[26] B. Zhang, G. Allegri, M. Yasaee and S. R. Hallett, "Micro-mechanical finite element analysis of Z-pins under mixed-mode loading," *Composites Part A: Applied Science and Manufacturing,* vol. 78, pp. 424-435, 2015.

[27] A. P. Mouritz, "Review of z-pinned composite laminates," *Composites Part A: Applied Science and Manufacturing*, vol. 38, pp. 2383-2397, 2007.

[28] M. Grassi and X. Zhang, "Finite element analyses of mode I interlaminar delamination in z-fibre reinforced composite laminates," *Composites Science and Technology*, vol. 63, pp. 1815-1832, 2003.

[29] D. J. Barrett, "The mechanics of z-fiber reinforcement," *Composite Structures*, vol. 36, pp. 23-32, 1996.

[30] M. Colin de Verdiere, A. K. Pickett, A. A. Skordos and V. Witzel, "Effect of tufting on the response of non-crimp fabric composites," in *ECCOMAS Thematic Conferance on Mechanical Response of Composites*, Porto, Portugal, 2007.